

INFLUENCES OF LOVASTATIN ON MEMBRANE ION FLOW AND INTRACELLULAR SIGNALING IN BREAST CANCER CELLS

NA WEI, MAN TIAN MI* and YONG ZHOU

Department of Nutrition and Food Hygiene, Third Military Medical University,
Chongqing 400038, P.R. China

Abstract: Lovastatin, an inhibitor of cellular cholesterol synthesis, has an apparent anti-cancer property, but the detailed mechanisms of its anti-cancer effects remain poorly understood. We investigated the molecular mechanism of Lovastatin anti-tumor function through the study of its effect on membrane ion flow, gap junctional intercellular communication (GJIC), and the pathways of related signals in MCF-7 mammary cancer cells. After treatment for 24-72 h with 4, 8 or 16 $\mu\text{mol/L}$ Lovastatin, cellular proliferation was examined via the MTT assay, and changes in membrane potential and cellular $[\text{Ca}^{2+}]_i$ were monitored using confocal laser microscopy. In addition, the expression of plasma membrane calcium ATPase isoform 1 (PMCA1) mRNA was analyzed via RT-PCR, the GJIC function was examined using the scrape-loading dye transfer (SLDT) technique, and MAPK phosphorylation levels were tested with the kinase activity assay. The results showed that Lovastatin treatment significantly inhibited the growth of MCF-7 breast cancer cells. It also increased the negative value of the membrane potential, leading to the hyperpolarization of cells. Moreover, Lovastatin treatment continuously enhanced $[\text{Ca}^{2+}]_i$, although the levels of PMCA1 mRNA were unchanged. GJIC was also upregulated in MCF-7 cells, with transfer of LY Fluorescence reaching 4 to 5 rows of cells from the scraped line after treatment with 16 $\mu\text{mol/L}$ Lovastatin for 72 h. Finally, downregulation of ERK1 and p38^{MAPK} phosphorylation were found in Lovastatin-treated MCF-7 cells. It could be deduced that Lovastatin can induce changes in cellular hyperpolarization and intracellular Ca^{2+} distributions, and increase GJIC function. These effects may result in changes in the downstream signal cascade, inhibiting the growth of MCF-7 cells.

* Author for correspondence: e-mail: mimt@vip.sina.com

Abbreviations used: $[\text{Ca}^{2+}]_i$ – cytosolic free Ca^{2+} concentration; GI – growth inhibition; GJIC – gap junctional intercellular communication; HMG-CoA – 3-hydroxy-3-methylglutaryl-coenzyme A; LOV – lovastatin, MVA – mevalonic acid; PMCA1 – plasma membrane calcium ATPase isoform 1

Key words: Lovastatin, Human breast cancer cells, Cellular membrane ion transfer, Gap junctional intercellular communication (GJIC), MAPK activity

INTRODUCTION

The cell membrane is the primary barrier between the intra- and extracellular environments, and it plays important roles in cellular activation and proliferation. Cholesterols, the main components of mammalian cellular membranes, are necessary for cell growth and proliferation, and are required for normal cellular activity. Endogenous cholesterol synthesis is regulated by 3-hydroxy-3-methylglutaryl-coenzyme A (HMG-CoA) reductase, while exogenous cholesterol is added to the cell membrane via intake by the low-density lipoprotein receptors (LDL-R). Endogenous and exogenous cholesterols interact with each other to maintain a relatively stable cholesterol level within the cell [1]. Indeed, research has shown that cholesterol depletion can lead to phenotypic changes and inhibition of cell growth [2].

Lovastatin (LOV) and other statins, commonly used to lower blood-lipid levels, are inhibitors of HMG-CoA reductase. They can lower endogenous cellular cholesterol synthesis, and block the mevalonate (MVA) metabolic pathway, the end products of which (cholesterols, dolichol, coenzyme Q, isoamylene proteins, etc.) are necessary components of the cell membranes. Consequently, inhibition of the MVA metabolic pathway not only blocks neogenesis of membrane lipids, but also impacts on membrane electron transfer and modifies Ras superfamily members. In addition, LOV was recently assessed as a possible anti-tumor drug that might inhibit tumor cell proliferation, or induce tumor cell differentiation, maturity or apoptosis [3, 4]. Maintenance of normal membrane structure is vital to membrane functions such as ion flow across cellular membranes and intercellular communication. Cellular proliferation and differentiation, demonstrating membrane potential, cytosolic free Ca^{2+} concentration ($[\text{Ca}^{2+}]_i$), gap junctional intercellular communication (GJIC) [5] and intracellular signal transmission are all closely related to the structure and function of cellular membranes and the membrane framework. It is therefore important to understand the impact of LOV on the membranes of normal and cancerous cells. In this study, we investigated the molecular mechanism of LOV anti-tumor function through assessments of its effect on the ion flow across membranes, GJIC, and the pathways of related signals in MCF-7 mammary cancer cells.

MATERIALS AND METHODS

Reagents

Lovastatin (Fluka Company, Switzerland) was dissolved in dimethyl sulfoxide (DMSO, Sigma) to a stock concentration of $3.2 \times 10^4 \mu\text{mol/L}$ and stored at -20°C . The final concentrations for cell treatments were 4, 8 and $16 \mu\text{mol/L}$. The fluorescent probes diS-C3-(5) (3,3'-dipropylthiadicarbocyanine iodide) and Pluronic F-127 were obtained from Molecular Probes Inc. (Eugene, OR, USA).

Fluo-3/AM and Lucifer Yellow CH were obtained from Sigma (USA). 1.0% Fluo-3/AM was dissolved in DMSO, diluted to 1 mmol/L and stored at 4°C. Lucifer Yellow CH stock solution was diluted to 1.0% in PBS and stored at 4°C in the dark. Goat anti-ERK1 and rabbit anti-p38^{MAPK} polyclonal Ab were obtained from Santa Cruz Biotechnology, Inc. (Santa Cruz, CA, USA) and diluted 1:250 before use. [γ -32P]ATP was purchased from Beijing Yahui Biomedical Engineering Company (Beijing, China).

Cell cultures

The mammary cancer cell line MCF-7 was obtained from the Shanghai Institute of Cell Biology of the Chinese Academy of Sciences (Shanghai, China). Cells were cultured in DMEM/F12 (Hyclone, USA) supplemented with 10% heat-inactivated fetal bovine serum (FBS; Hyclone USA), 1.2 g sodium bicarbonate, 100 μ g/ml streptomycin and 100 U/ml penicillin at 37°C in a humidified atmosphere of 5% CO₂.

Cell growth curve

Cells were seeded in 24-well plates at a density of 5.0×10^4 cells/ml, and treated with LOV at final concentrations of 4, 8 and 16 μ mol/L. Each group included three parallel wells. After 24-72 h, the cells were stained with trypan blue and counted, and cell growth inhibition was calculated as follows:

$$\text{Growth inhibition (GI)} = [(Nc - Nt) / Nc] \times 100\%$$

where Nc (Control group) and Nt (Treatment group) were cell counts at a given time point.

MTT assay

The cytostatic/cytotoxic effects of LOV on MCF-7 cells were tested via a standard MTT (3-(4,5-dimethylthiazol-2-yl)-2,5-diphenyl-tetrazolium bromide, Biomol USA) assay. Cells were plated out at a density of 5.0×10^4 cells/200 μ l/well in 96-well microtitre plates and allowed an overnight period for attachment. Then, the medium was removed and fresh medium along with various concentrations of LOV were added to the cultures in parallel. Control cells without agents were cultured under the same conditions with comparable medium changes. Following treatment, cells were fed with drug-free medium (200 μ l/well) and MTT (15 μ l/well, 5 mg per ml in PBS), and incubation was prolonged for 4 h at 37°C. After removing the supernatants, the MTT-formazan crystals were dissolved in dimethyl sulphoxide (200 μ l/well) for 30 min at room temperature, and the absorbance was measured at 492 nm in a universal microplate reader (Elx 800, BIO-TEK instruments, INC). The final medium concentration of DMSO was $\leq 0.05\%$ in the control and treatment groups.

Changes in cellular membrane potential

Changes in cellular membrane potential were examined using confocal microscopy with the fluorescent dye diS-C3-(5) [6-8]. Briefly, cells in the logarithmic growth phase were isolated and plated on coverslips in a 24-well

plate, and incubated overnight to allow adherence. Cells were then treated with LOV at 4, 8 and 16 $\mu\text{mol/L}$ for 24, 48 and 72 h, respectively, washed with PBS, and incubated with the membrane potential-sensitive fluorescent diS-C3-(5) probes at a final concentration of 1 $\mu\text{mol/L}$ for 30 min at 37°C. The cells were washed, and changes in the cellular membrane potential were examined using a Leica TCS NT-laser scanning confocal system. 100 cells were randomly chosen from different coverslips in each test group, and the cellular fluorescence intensity was analyzed using an image analysis system (TCS-Tools, Leica TCS-NT, Germany).

Changes in intracellular free calcium concentration

Cells were treated as described above, rinsed with DMEM medium, adhered to coverslips, and incubated with 0.5 ml DMEM containing 4 $\mu\text{mol/L}$ Fluo-3/AM and 1.0 μl 12.5% pluronic F-127 for 45 min at 37°C [9]. The coverslips were again rinsed with DMEM and used for laser scanning confocal microscopic examination, and 100 cells per test group were randomly chosen for cellular fluorescence intensity analysis.

Expression levels of plasma membrane calcium ATPase mRNA

The level of plasma membrane calcium ATPase 1 (PMCA1) mRNA expression in the MCF-7 cells was analyzed as described previously [10]. Briefly, for reverse transcription, 3 μg of RNA dissolved in 50 μl PCR-compatible buffer was combined with 50 μl of 2 \times RT Master Mix (10 μl of 10 \times reverse transcription buffer, 4 μl of 10mmol/L dNTPs, 10 μl of 10 \times random primers, 5 μl of multiscribe reverse transcriptase (50 U/ μl) and 21 μl of nuclease-free H₂O), and RT was performed at 37°C for 60 min, and then 72°C for 10 min. For PCR, 10 ng of cDNA was combined with primers and 2 \times SYBR Green PCR Master Mix to a final reaction volume of 50 μl . The nucleotide sequences for the different primer pairs were as follows:

PMCA1: forward primer 5'-TGGTGCAAATTCCATAGACATCTC-3', reverse primer 5'-GAGCTGCGGGCTCTCATG-3', producing an 88-bp amplification product;

Human β -actin: forward primer 5'-GGGTCAGAAGGATTCCTAATG-3', reverse primer 5'-GGTCTCAAACATGATCTGGG-3', amplified as an internal control, and with a PCR product 237 bp long.

PCR reactions were done at 95°C for 5 min, followed by 45 cycles at 94°C, 20 s, and 62°C, 1 min. Finally, the RT-PCR products were examined via 1.5% agarose gel electrophoresis to ensure that bands were visible only at the expected molecular weight.

Change in GJIC function

GJIC function changes were examined via the scrape-loading dye transfer method [11]. Briefly, cells were seeded into 35-mm dishes and fed to saturation density. The cells were treated with different doses of LOV for 24-72 h, then rinsed three times with PBS, then exposed to 0.05% Lucifer Yellow CH (Sigma). Scrape lines

were made with scrape blades. After 3 min, the dishes were rinsed three times with PBS, examined with a Nikon fluorescence microscope and photographed.

Western blot analysis of ERK1 and p38^{MAPK} protein expression

Cytosolic extracts were prepared using ice-cold Nonidet P-40 (NP-40) lysis buffer (50 mmol/L Tris-HCl pH 8.0, 150 mmol/L NaCl, 25 mmol/L NaF, 5 mmol/L Na₄P₂O₇, 0.1% NP-40, 10 µg/ml aprotinin, 10 µg/ml leupeptin, 1 mmol/L phenylmethylsulfonyl fluoride) and incubated on ice for 30 min. After centrifugation at 12,000 g for 15 min, the protein in the supernatants was quantitated by the Lowry method using bovine serum albumin (BSA) as a standard. Sixty micrograms of protein per lane was electrophoresed on 10% SDS-polyacrylamide gels. After transfer of the protein from the gel to nitrocellulose membranes, the membranes were blocked at 37°C for 1 h in PBS plus 0.1% Tween-20 (PBS-T) containing 1% BSA, then incubated for 1 h at 37°C with polyclonal antibodies against human ERK1 or human p38^{MAPK} antibody. Bound antibody was detected by chemiluminescence.

***In vitro* kinase assay for ERK and p38^{MAPK} activities**

Proteins (200 µg) were incubated for 4 h at 4°C with ERK1 or p38^{MAPK} polyclonal antibody (1 µg), then for 2 h at 4°C with protein A-Sepharose. MAPK kinase assays were performed for 30 min at 25°C on the bound immune complexes in a reaction buffer containing substrate protein (1mg/ml MBP), 40 µmol/L ATP and 2 µCi [γ -³²P]ATP. The level of ³²P penetrating the substrate protein (in pmol/mg/min) represented the ERK1 and p38^{MAPK} activities.

Statistical analysis

All the data was analyzed using SPSS software ver. 10.0. All the quantitative data was presented as the mean±standard error of three independent experiments. Statistical significance was assessed using variance analyses.

RESULTS

The effect of LOV on MCF-7 cell growth

The MTT assay showed that after 24-72 hours of treatment with 4-16 µmol/L LOV, the A492 values of the treated group had all declined in a dose- and time-dependent manner compared to the controls (Fig. 1). From the formula for growth inhibition (GI), we found that GI increased from 5.57 to 42.42% and 17.39 to 75.80% with increasing time after treatment with, respectively, 4 and 16 µmol/L LOV (Fig. 2).

Changes in membrane potential as observed by laser confocal microscopy

The quantity of diS-C₃-(5) in cells can directly reflect changes in membrane potential: hyperpolarization of cells increases the partitioning of this positively-charged dye into the lipid phase of the membrane and cytoplasm [6], where its fluorescence is quenched, while its fluorescence intensifies in the opposite case. In

this study, after the treatment with 4, 8 or 16 $\mu\text{mol/L}$ LOV, the quantity of diS-C₃-(5) in MCF-7 cells was observed to gradually decline (Fig. 3). This illustrated that within the cells, LOV treatment resulted in an increase in the negative value of membrane potential and a change in the cells' hyperpolarization. Even at the lowest dose (4 $\mu\text{mol/L}$ LOV for 24 h), cellular diS-C₃-(5) fluorescence decreased significantly ($P < 0.01$). The response intensified thereafter in a dose- and time-dependent manner.

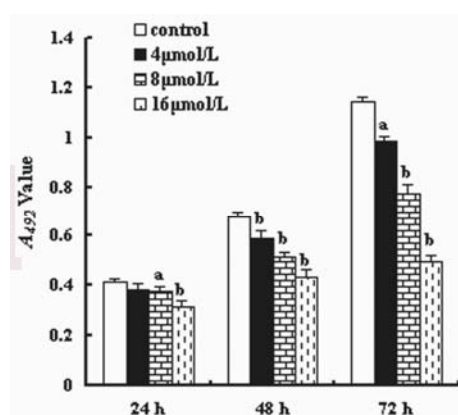


Fig. 1. The effect of LOV on the proliferation of MCF-7 cells. After treatment with various concentrations of LOV for 24-72 h, cells were incubated with MTT, and the MTT-formazan crystals were measured at 492 nm in a universal microplate reader. Note: a indicates $P < 0.05$ vs. the control group; b indicates $P < 0.01$ vs. the control group.

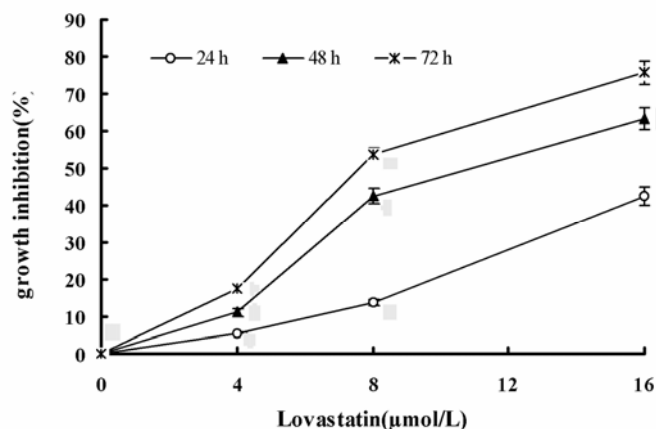


Fig. 2. Changes in GI in MCF-7 cells. Different concentrations of LOV were incubated for 24-72 h with MCF-7 cells (5.0×10^4 cells/ml). After treatment, cells were counted via the trypan blue method, and the cell growth inhibition was calculated.

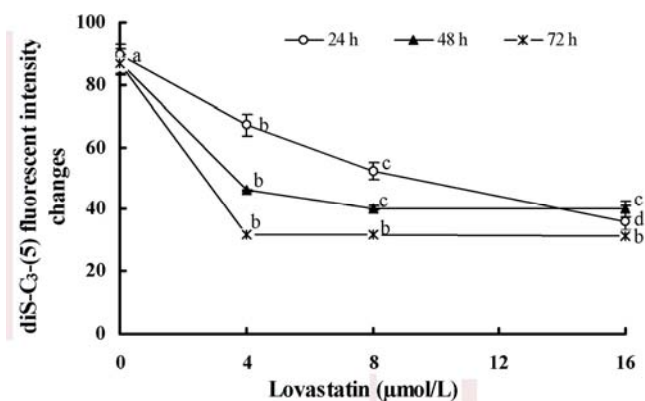


Fig. 3. The fluorescence intensity change of diS-C₃-(5) in MCF-7 cells. After treatment with LOV, the cells were incubated with 1 μmol/L diS-C₃-(5) for 30 min at 37°C, and changes in the cellular membrane potential were examined using a Leica TCS NT-laser scanning confocal system. 100 cells were randomly chosen from different coverslips in each test group, and the cellular fluorescence intensity was analyzed using an image analysis system. Note: values with a different letter on a given curve differ significantly ($P < 0.05$).

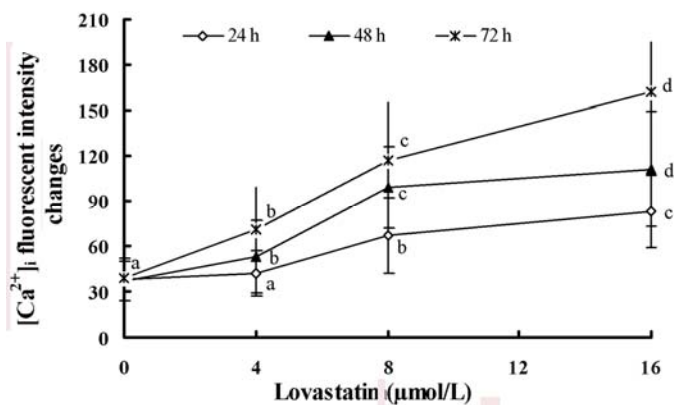


Fig. 4. Fluorescence intensity changes in the intracellular free calcium concentration in MCF-7 cells. After treatment with LOV, cells were incubated with 0.5 ml DMEM containing 4 μmol/L Fluo-3/AM and 1.0 μl 12.5% pluronic F-127 for 45 min at 37°C. After a rinse with DMEM, changes in [Ca²⁺]_i were examined with a laser scanning confocal microscope. 100 cells per test group were randomly chosen, and the cellular fluorescence intensity was analyzed using an image analysis system. Note: values with a different letter on a given curve differ significantly ($P < 0.05$).

The effect of LOV on intracellular Ca^{2+} concentration and PMCA1 mRNA expression

MCF-7 cells were treated with 4-16 $\mu\text{mol/L}$ LOV for 24-72 hours and examined using laser confocal scanning microscopy. We found that the intracellular fluorescence intensity had strengthened in the test groups, indicating that the $[\text{Ca}^{2+}]_i$ had increased. Furthermore, the higher the dosage of LOV and the longer the treatment time, the more obvious the effect became (Fig. 4), demonstrating a time- and dose-dependent relationship. RT-PCR analysis showed that PMCA1 mRNA expression in the MCF-7 cells did not change following LOV treatment (Fig. 5), suggesting that this increase in free Ca^{2+} was not due to up-regulated gene expression of calcium ATPase or elevated release of Ca^{2+} from the Ca^{2+} pool. It may have been due to the changed activity of calcium ATPase because of an abnormality in the membrane structure and function after LOV treatment.

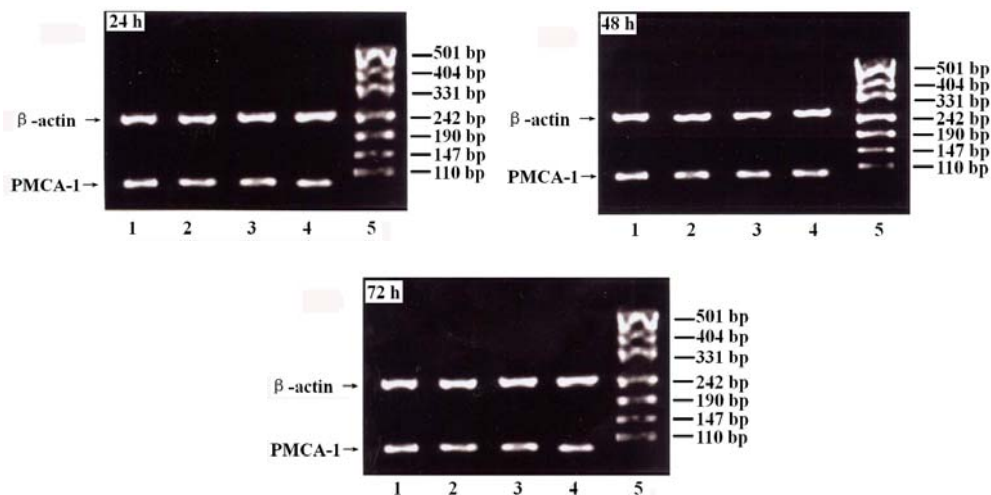


Fig. 5. The effect of LOV on the expression of PMCA1 mRNA in MCF-7 cells. MCF-7 cells grown to about 70% confluence were treated with 4, 8 or 16 $\mu\text{mol/L}$ LOV for the indicated time period, while the control cells received 0.05% DMSO only. PMCA1 expression was analyzed by RT-PCR. Lane 1: 16 $\mu\text{mol/L}$ group; lane 2: 8 $\mu\text{mol/L}$ group; lane 3: 4 $\mu\text{mol/L}$ group; lane 4: control group; lane 5: DNA molecular marker.

The effect of LOV on GJIC function

In the control assays, cellular LY fluorescent dye was unable to transfer to adjacent cells, instead remaining on the sides of scrape lines, which is consistent with negative GJIC function. After 24-72 hours treatment with 4, 8, or 16 $\mu\text{mol/L}$ LOV, MCF-7 cells showed a time- and dose-dependent activation of GJIC to the point that the LY dye was transmitted 4-5 cell layers deep in some cases (Fig. 6 A-D, Tab. 1).

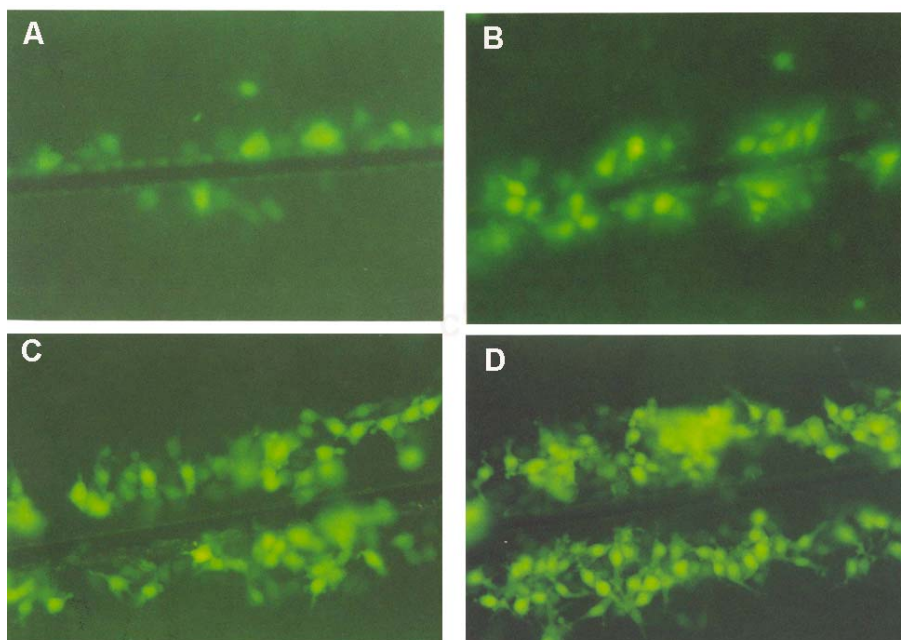


Fig. 6. The changes in the GJIC of MCF-7 cells incubated with 16 $\mu\text{mol/L}$ LOV for 24-72 h (B-D), then exposed to 0.05% Lucifer Yellow CH. The control group is shown in A. After 3 min, the cells were rinsed with PBS, examined with a Nikon fluorescence microscope and photographed.

Tab. 1. The effect of LOV on MCF-7 GJIC.

Group	24 h	48 h	72 h
Control	–	–	–
4 $\mu\text{mol/L}$	–	+	++
8 $\mu\text{mol/L}$	+	++	+++
16 $\mu\text{mol/L}$	+	+++	++++

Note: – indicates LY Fluorescence was limited to the cells of the scrape lines; + ~ ++++ indicate LY fluorescence reached 2 (+) to 5 (++++) rows of cells from the scraped line. See Fig. 6.

Changes in the expression and activation of ERK1 and p38^{MAPK}

Following 48-72 h exposure to LOV, western blot analysis showed that the levels of ERK1 were unchanged (Fig. 7). The expression of p38^{MAPK} was clearly down-regulated after 72 h exposure to the drug (Fig. 7). Interestingly, the assay of kinase activation (Fig. 8) revealed that ERK1 and p38^{MAPK} phosphorylation levels were both markedly decreased compared to the control ($P < 0.05$). This was most obvious in cells treated with 16 $\mu\text{mol/L}$ LOV ($P < 0.01$).

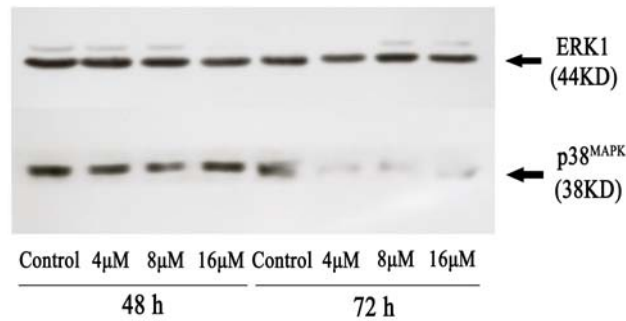


Fig. 7. The effect of LOV on ERK1 and p38^{MAPK} expression in MCF-7 cells. The cells were incubated for 48-72 h with 4, 8 or 16 μmol/L LOV, then total proteins were extracted and separated by SDS-PAGE. After transfer, the membrane was probed with antibodies reacting with ERK1 or p38^{MAPK}, and the bound antibodies were detected by chemiluminescence.

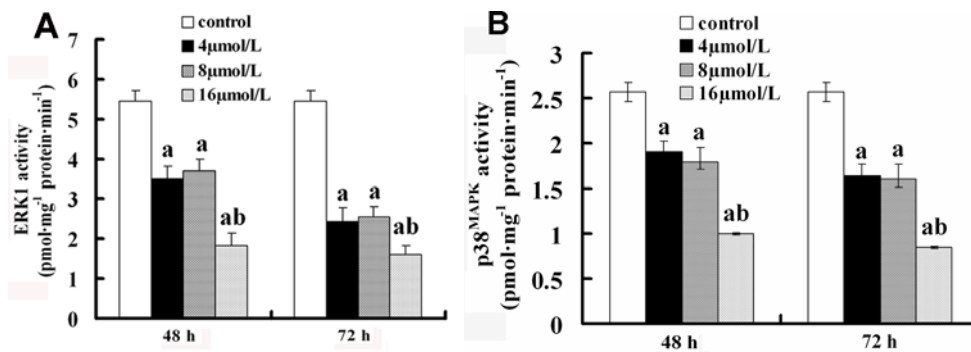


Fig. 8. The change in ERK1 (A) and p38^{MAPK} (B) activity in MCF-7 cells treated with LOV. The cell protein extracts, untreated or treated with LOV for 48-72 h, were incubated with goat anti-ERK1 or rabbit anti-p38^{MAPK} polyclonal Ab, and the immune complexes were adsorbed on Protein A Sepharose; then ERK1 and p38^{MAPK} kinase activity was assayed by using [γ -³²P]ATP and substrate protein. Note: a indicates $P < 0.05$ vs. the control group; b indicates $P < 0.05$ vs. the 4 μmol/L and 8 μmol/L groups.

DISCUSSION

Cholesterol is the main component of the cell membrane, and it plays an important role in maintaining normal membrane structure and function. An imbalance in the tightly regulated relationship between cellular sterols and other lipids can lead to membrane lipid microenvironment changes that may affect the biophysical features of the membrane, including membrane potential, membrane

lipid fluidity, ion permeability and signal transmission [12]. Lovastatin (LOV), one of the drugs used to treat hyperlipidemia, can lower the level of endogenous cellular cholesterol synthesis by inhibiting the activity of HMG-CoA reductase. Recent studies have demonstrated that LOV has a potential anti-cancer property [3, 4], but researchers have yet to reach a comprehensive understanding of the molecular mechanisms of its anti-cancer action. LOV may affect cellular proliferation and differentiation by altering the structure and function of cellular membranes and signal transmission.

Membrane potential is one of the most important biophysical features of the cell membrane. DiS-C₃-(5) [6, 7] is a lipophilic cation fluorescent dye, and it can be used to quickly and accurately assess changes in membrane potential [7, 8, 13-15]. Our experiments showed that when the exogenous LOV inhibited cholesterol synthesis and the MVA metabolic pathway, the amount of diS-C₃-(5) fluorescence decreased in a dose- and time-dependent manner. The differences were significant at all the tested times and doses. This shows that LOV can effectively enlarge the negative value of the membrane potential of MCF-7 cells. We speculate that LOV might act by inhibiting the synthesis of cellular endogenous cholesterol, by interfering in the MVA metabolism pathway to change the cellular membrane structure and even membrane protein functions, leading to cellular hyperpolarization. Interestingly, such hyperpolarization can affect cell proliferation [16], and many studies have demonstrated that LOV can suppress tumor cell proliferation by arresting the cell cycle in the G0/G1 phase [17, 18]. In this study, we also found that LOV inhibited MCF-7 cell proliferation and enhanced GI as time and dose increased, suggesting these effects may be closely related to the hyperpolarization of MCF-7 cells.

Ca²⁺ is an important signal transduction ion in cells and it plays a significant role in regulating vital cellular activities. Under normal conditions, the Ca²⁺ concentration in cells is lower than that outside cells. Homeostasis of a lower Ca²⁺ concentration across cellular membranes is the key to maintaining normal cellular function. Indeed, many studies have shown that increasing [Ca²⁺]_i in tumor cells is an important function of many anti-tumor drugs, as it inhibits tumor cell proliferation or initiates apoptosis [19, 20]. Thus, artificial increases in [Ca²⁺]_i in tumor cells are an important and effective mode of cancer treatment [21, 22]. In investigating LOV, an anti-cholesterol drug with possible anti-cancer applications, we found that LOV inhibited MCF-7 breast cancer cell proliferation in association with an increase in [Ca²⁺]_i. However, LOV did not affect the mRNA expression of PMCA1 [10], which is the primary calcium pump on the membrane surface of MCF-7 cells. It is possible that LOV might change the physical properties of lipid bilayer and protein functions in the plasma membrane, thus affecting PMCA1 activities leading to the observed increase in [Ca²⁺]_i. Therefore, these increases in [Ca²⁺]_i may change downstream signaling, resulting in the observed inhibition effects of LOV on MCF-7 cell proliferation.

GJIC plays significant roles in embryonic development, cell growth, differentiation, apoptosis, and the coordination of many other intercellular activities via the exchange of small molecules such as calcium ions, IP₃, and cAMP between the linked cells [23-25]. The structural unit of the gap junctions is connexon, a plasma membrane protein composed of six transmembrane subunits. Research has revealed a GJIC disorder in almost all parenchymal tumor tissues, in which signal transmission was completely disrupted between adjacent tumor cells, and between tumor cells and the surrounding normal cells. In addition, varying degrees of disruption of GJIC function have been reported for cells in the process of transforming to cancer cells [26-28], and the restoration of GJIC can suppress tumor cell growth. Many anti-cancer or chemopreventive and chemotherapeutic chemicals have been shown to either prevent the down-regulation of GJIC or up-regulate GJIC [29]. In our study, we found that while LOV inhibited MCF-7 cell proliferation, it also recovered or upregulated cellular GJIC in a dose- and time-dependent manner, suggesting a promotion of GJIC by LOV in MCF-7 cells, possibly via a change in the membrane lipid composition and membrane protein functions through the HMG-CoA reductase pathway.

At the same time, the MAPK pathway, another important signal system that regulates cell proliferation and cell differentiation, was affected by LOV treatment [30-32]. Our study showed that treatment with LOV did not alter the total ERK1 protein levels in MCF-7 cancer cells, but markedly inhibited ERK1 activity and p38^{MAPK} protein phosphorylation, as in previous findings [33]. This suggests that the MAPK signal transducing phosphorylation cascade was regulated at least partially in an MVA-dependent manner, and the influences of the drug were a consequence of its inhibitory effects on the synthesis of steroids [34-35]. Moreover, this indicates that by changing membrane function, LOV treatment affects membrane-related MAPK cellular signal pathways, which may play an important role in inhibiting MCF-7 cell proliferation.

In summary, this study demonstrates that LOV, as an inhibitor of cellular cholesterol synthesis, may change membrane lipid composition in MCF-7 cells, thereby affecting the structures and activities of ion channel proteins and gap junctional proteins in the cellular membrane. This results in the induction of cellular hyperpolarization change, intracellular calcium overload, and intercellular communications restoration. All these changes, accompanied by alterations of intracellular signal transduction and subsequent changes in the cellular metabolism, lead to the observed inhibition effect on MCF-7 breast cell proliferation.

Acknowledgments. The research project was financially supported by grant 30271128 funded by the National Nature Science Foundation of China.

REFERENCES

1. Lange, Y., Duan, H. and Mazzone, T. Cholesterol homeostasis is modulated

- by amphiphiles at transcriptional and post-transcriptional loci. **Lipid Res.** 37 (1996) 534-539.
2. Buttke, T.M. and Van Cleave, S. Adaptation of a cholesterol deficient human T cell line to growth with lanosterol. **Biochem. Biophys. Res. Commun.** 200 (1994) 206-212.
 3. Shellman, Y.G., Ribble, D., Miller, L., Gendall, J., Vanbuskirk, K., Kelly, D., Norris, D.A. and Dellavalle, R.P. Lovastatin-induced apoptosis in human melanoma cell lines. **Melanoma Res.** 15 (2005) 83-89.
 4. Dimitrowlakos, J., Ye, L.Y., Benzaquen, M., Moore, M.J., Kamel-Reid, S., Freedman, M.H., Yeger, H. and Penn, L.Z. Differentiation sensitivity of various pediatric cancers and squamous cell carcinomas to Lovastatin-induced apoptosis: therapeutic implications. **Clin. Cancer Res.** 7 (2001) 158-167.
 5. Ruch, R.J., Madhukar, B.V., Trosko, J.E. and Klaunig, J.E. Reversal of ras-induced inhibition of gap-junctional intercellular communication, transformation, and tumorigenesis by lovastatin. **Mol. Carcinog.** 7 (1993) 50-59.
 6. Hladky, S.B. and Rink, T.J. Potential difference and the distribution of ions across the human red blood cell membrane; a study of the mechanism by which the fluorescent cation, diS-C₃-(5) reports membrane potential. **J. Physiol.** 263 (1976) 287-319.
 7. Plasek, J. and Hronda, V. Assessment of membrane potential changes using the carbocyanine dye, diS-C₃-(5): synchronous excitation spectroscopy studies. **Eur. Biophys. J.** 19 (1991) 183-188.
 8. Suzuki, H., Wang, Z.Y., Yamakoshi, M., Kobayashi, M. and Nozawa, T. Probing the transmembrane potential of bacterial cells by voltage-sensitive dyes. **Anal. Sci.** 19 (2003) 1239-1242.
 9. Kao, J.P., Harootunian, A.T. and Tsien, R.Y. Photochemically generated cytosolic calcium pulses and their detection by Fluo-3. **J. Biol. Chem.** 264 (1989) 8179-8184.
 10. Roberts-Thomson, S.J., Holman, N.A., May, F.J., Lee, W.J. and Monteith, G.R. Development of a real-time RT-PCR assay for plasma membrane calcium ATPase isoform 1 (PMCA1) mRNA levels in a human breast epithelial cell line. **J. Pharmacol. Toxicol. Methods** 44 (2000) 513-517.
 11. el-Fouly, M.H., Trosko, J.E. and Chang, C.C. Scrape-loading and dye transfer. A rapid and simple technique to study gap junctional intercellular communication. **Exp. Cell Res.** 168 (1987) 422-430.
 12. Zhuang, L., Kim, J., Adam, R.M., Solomon, K.R. and Freeman, M.R. Cholesterol targeting alters lipid raft composition and cell survival in prostate cancer cells and xenografts. **J. Clin. Invest.** 115 (2005) 959-968.
 13. Waczulikova, I., Sikurova, L., Bryszewska, M.R., Kawiecka, K., Carsky, J. and Ulicna, O. Impaired erythrocyte transmembrane potential in diabetes mellitus and its possible improvement by resorcylicidene aminoguanidine. **Bioelectrochemistry** 52 (2000) 251-256.

14. Toyomizu, M., Okamoto, K., Akiba, Y., Nakatsu, T. and Konishi, T. Anacardic acid-mediated changes in membrane potential and pH gradient across liposomal membrane. **Biochem. Biophys. Acta** 1558 (2002) 54-62.
15. de Poorter, L.M. and Keltjens, J.T. Convenient fluorescence-based methods to measure membrane potential and intracellular pH in the Archaeo Methanobacterium thermoautotrophicum. **J. Microbiol. Methods** 47 (2001) 233-241.
16. Schiffenbauer, Y.S., Trubniykov, E., Zacharia, B.T., Gerbat, S., Rehavi, Z., Berke, G. and Chaitchik, S. Tumor sensitivity to anti-cancer drugs predicted by changes in fluorescence intensity and polarization *in vitro*. **Anticancer Res.** 22 (2002) 2663-2669.
17. Fouty, B.W. and Rodman, D.M. Mevastatin can cause G1 arrest and induce apoptosis in pulmonary artery smooth muscle cells through a p27Kip1-independent pathway. **Circ. Res.** 92 (2003) 501-509.
18. Germano, D., Pacilio, C., Cancemi, M., Cicatiello, L., Altucci, L., Petrizzi, V.B., Sperandio, C., Salzano, S., Michalides, R.J., Taya, Y., Bresciani, F. and Weisz, A. Inhibition of human breast cancer cell growth by blockade of the mevalonate-protein prenylation pathway is not prevented by overexpression of cyclin D1. **Breast Cancer Res. Treat.** 67 (2001) 23-33.
19. Zhang, T.C., Cao, E.H., Li, J.F., Ma, W. and Qin, J.F. Induction of apoptosis and inhibition of human gastric cancer MGC-803 cell growth by arsenic trioxide. **Eur. J. Cancer** 35 (1999) 1258-1263.
20. Florio, T., Thellung, S., Arena, S., Corsaro, A., Spaziante, R., Gussoni, G., Acuto, G., Giusti, M., Giordano, G. and Schettini, G. Somatostatin and its analog lanreotide inhibit the proliferation of dispersed human non-functioning pituitary adenoma cells *in vitro*. **Eur. J. Endocrinol.** 141 (1999) 396-408.
21. Miyake, H., Hara, I., Yamanaka, K., Arakawa, S. and Kamidono, S. Calcium ionophore, ionomycin inhibits growth of human bladder cancer cells both *in vitro* and *in vivo* with alteration of Bcl-2 and Bax expression levels. **J. Urol.** 162 (1999) 916-921.
22. Popescu, B.O., Cedazo-Minguez, A., Popescu, L.M., Winblad, B., Cowburn, R.F. and Ankarcrna, M. Caspase cleavage of exon 9 deleted presenilin-1 is an early event in apoptosis induced by calcium ionophore A 23187 in SH-SY5Y neuroblastoma cells. **J. Neurosci. Res.** 66 (2001) 122-134.
23. Cronier, L., Frenedo, J.L., Defamie, N., Pidoux, G., Bertin, G., Guibourdenche, J., Pointis, G. and Malassine, A. Requirement of gap junctional intercellular communication for human villous trophoblast differentiation. **Biol. Reprod.** 69 (2003) 1472-1480.
24. Evans, W.H. and Martin, P.E. Gap junctions: Structure and Function. **Mol. Membr. Biol.** 19 (2002) 121-136.
25. Alexander, D.B. and Goldberg, G.S. Transfer of biologically important molecules between cells through gap junction channels. **Curr. Med. Chem.** 10 (2003) 2045-2058.

26. Carruba, G., Webber, M.M., Quader, S.T., Amoroso, M., Cocciadiferro, L., Saladino, F., Trosko, J.E. and Castagnetta, L.A. Regulation of cell-to-cell communication in non-tumorigenic and malignant human prostate epithelial cells. **Prostate** 50 (2002) 73-82.
27. Saito, T., Tanaka, R., Wataba, K., Kudo, R. and Yamasaki, H. Overexpression of estrogen receptor-alpha gene suppresses gap junctional intercellular communication in endometrial carcinoma cells. **Oncogene** 23 (2004) 1109-1116.
28. Trosko, J.E. and Ruch, R.J. Cell-cell communication in carcinogenesis. **Front Biosci.** 3 (1998) D208-236.
29. Trosko, J.E. and Ruch, R.J. Gap junctions as targets for cancer chemoprevention and chemotherapy. **Curr. Drug Targets** 3 (2002) 465-482.
30. Van Golen, K.L., Bao, L.W., Pan, Q., Miller, F.R., Wu, Z.F. and Merajver, S.D. Mitogen activated protein kinase pathway is involved in RhoC GTPase induced motility, invasion and angiogenesis in inflammatory breast cancer. **Clin. Exp. Metastasis** 19 (2002) 301-311.
31. Senokuchi, T., Matsumura, T., Sakai, M., Yano, M., Taguchi, T., Matsuo, T., Sonoda, K., Kukidome, D., Imoto, K., Nishikawa, T., Kim-Mitsuyama, S., Takuwa, Y. and Araki, E. Statins suppress oxidized low density lipoprotein-induced macrophage proliferation by inactivation of the small G protein-p38 MAPK pathway. **J. Biol. Chem.** 280 (2005) 6627-6633.
32. Wu, J., Wong, W.W., Khosravi, F., Minden, M.D. and Penn, L.Z. Blocking the Raf/MEK/ERK pathway sensitizes acute myelogenous leukemia cells to lovastatin-induced apoptosis. **Cancer Res.** 64 (2004) 6461-6468.
33. Holstein, S.A. and Hohl, R.J. Interaction of cytosine arabinoside and lovastatin in human leukemia cells. **Leukemia Res.** 25 (2001) 651-660.
34. Johnson, M.D., Woodard, A., Okediji, E.J., Toms, S.A. and Allen, G.S. Lovastatin is a potent inhibitor of meningioma cell proliferation: evidence for inhibition of a mitogen associated protein kinase. **J. Neurooncol.** 56 (2002) 133-142.
35. Takata, R., Fukasawa, S., Hara, T., Nakajima, H., Yamashina, A., Yanase, N. and Mizuguchi, J. Cerivastatin-induced apoptosis of human aortic smooth muscle cells through partial inhibition of basal activation of extracellular signal-regulated kinases. **Cardiovasc. Pathol.** 13 (2004) 41-48.